DNA Devices

A Protein-Driven DNA Device That Measures the Excess Binding Energy of Proteins That Distort DNA**

*Wanqiu Shen, Michael F. Bruist, Steven D. Goodman, and Nadrian C. Seeman**

Nanomechanical devices hold the promise of controlling structure and performing exquisitely fine measurements on the molecular scale. We previously have reported three nanoscale devices that were built from DNA. The first device[1] extrudes or withdraws a portion of a DNA cruciform from a cyclic molecule in response to the presence of an intercalator. The second device is powered by the B–Z transition:[2] it switches a DNA domain from one side of a double-helical shaft to the other in response to the presence or absence of $[Co(NH_3)_6]^{3+}$ in its environment. The third device is sequence-dependent;[3] it changes structure as a function of DNA strands that are in solution with it. All of these devices change their states in response to an external stimulus, but they do not report new information about any other molecular system. Here we describe a new DNA device that changes shape when a DNA-distorting protein is added to the system. In this case, we used *E. coli* integration host factor (IHF), which bends DNA significantly when it binds to an appropriate recognition site.[4] Thus, we have developed a nanomechanical device for which the stimulus is a protein. However, this device does not merely have a different kind of activation signal. A second part of the device contains a series of nucleotide pairs that must be disrupted when the device is distorted by IHF. Consequently, this is a measuring device that enables us to estimate the amount of additional work that the protein can do when it binds to DNA.

Our IHF-activated device is illustrated schematically in Figure 1. This diagram does not illustrate the part of the device involved in measuring the work, but, for simplicity, shows just the way in which the binding of IHF to its target site can distort the relationship between two DNA triple crossover (TX) motifs that flank the binding site. The upper panel shows the DNA molecule in the absence of IHF: two previously characterized TX molecules[5] are connected by a DNA double-helical shaft; each TX molecule creates a stiff domain that rigidly transmits motions of the shaft on one side to the dyes on the other side. The shaft contains the λH1

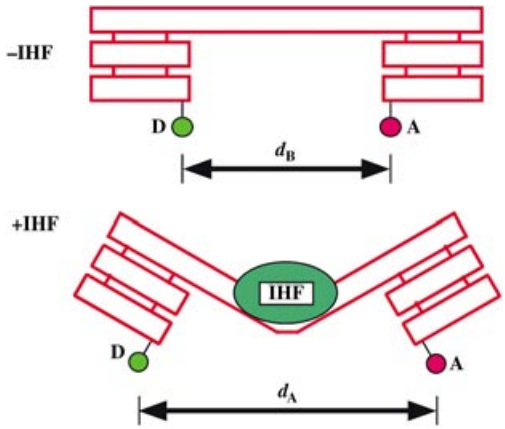

Figure 1. The action of the nanomechanical device. Double-helical DNA is shown as rectangular boxes. The triple crossover motifs (TX) are shown as three fused rectangular boxes. The upper domain connects the two TX motifs with the binding site for IHF. IHF is shown as a green ellipse, and in the lower panel its binding distorts the connecting shaft. For clarity, the 160° bend[4] is reduced to 45° here. A donor dye (D, fluorescein) and an acceptor dye (A, Cy3) are shown as a green and a magenta circle, respectively. The fluorescence resonance energy transfer reported by this pair decreases upon IHF binding, as the distance between the dyes increases from d_B to d_A.

[*] Dr. W. Shen, Prof. N. C. Seeman
Department of Chemistry
New York University
New York, NY 10003 (USA)
Fax: (+1) 212-260-7905
E-mail: ned.seeman@nyu.edu
Prof. M. F. Bruist
Department of Chemistry
University of the Sciences in Philadelphia
Philadelphia, PA 19104 (USA)
Prof. S. D. Goodman
Department of Molecular and Computational Biology
University of Southern California
Los Angeles, CA 90089-0641 (USA)

[**] We thank Dr. Paul Rothemund, Dr. Bruce Demple, and Dr. Alexander Vologodskii for valuable suggestions, and Dr. John SantaLucia for generously giving us prepublication estimates of stacking free energies. This research has been supported by grants GM-29554 from NIGMS, N00014-98-1-0093 from ONR, grants DMI-0210844, EIA-0086015, DMR-01138790, and CTS-0103002 from the NSF, F30602-01-2-0561 from DARPA/AFSOR to N.C.S. and GM-055392 from NIGMS to S.D.G.

 © 2004 Wiley-VCH Verlag GmbH & Co. KGaA, Weinheim DOI: 10.1002/ange.200460302

binding site[6] for IHF; the binding site is completely contained on the shaft, and does not extend past it to the TX molecules. Pendent from the bottom domains of the TX molecules are a pair of fluorescent dyes that are close enough (distance d_B) for energy to transfer between them, thus leading to a fluorescence resonance energy transfer (FRET) signal. The lower panel illustrates the effect of binding IHF to the molecule: it is distorted, which leads to an increase in the distance between the dyes (d_A) and a corresponding decrease in the FRET signal. This system is similar to that used in the B–Z device reported earlier, except that the change in energy transfer is now a consequence of DNA bending, rather than rotary displacement of a DNA double-crossover (DX) molecule.

Figure 2 illustrates the operation of the measuring device. The system is similar to that shown in Figure 1, but the lower domains of the TX portions of the device are now connected by a pair of cohesive strands (upper panel). The cohesion is broken when IHF binds to its recognition site on the top domain (lower panel). If an excess of free energy is available when IHF binds, it can disrupt the base pairs and bind normally. By using a range of cohesive lengths, each with a different free energy of association, one can use the nanodevice to estimate the amount of work of which IHF is capable when it binds to DNA. Figure 3 shows the sequence of the device. All devices used in this study migrate identically on nondenaturing gels, with mobilities similar to that of a topologically closed standard (data not shown).[7]

Figure 4 contains bar graphs that show the results of our experiments monitoring energy transfer from donor quenching; similar results are obtained from acceptor fluorescence (data not shown). In the first experiment, we took a given sequence of DNA [5′-TGCATCAC/TC-3′, where the slash

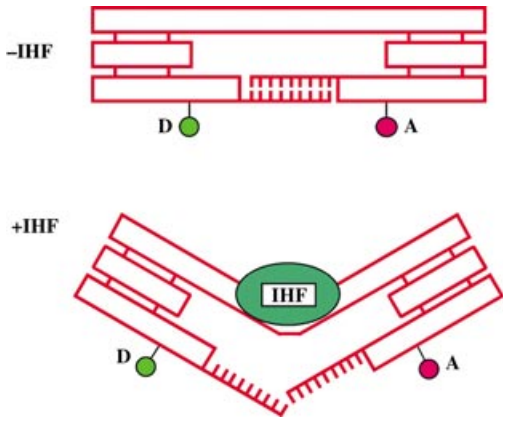

Figure 2. The TX-based measuring device. The diagram is similar to Figure 1, and the conventions there apply. However, the bottom domains have been extended towards each other, and they are connected by a cohesive tract. IHF must do work to separate the two strands in proportion to the length of the cohesive tract. Increasing the length of the cohesive tract leads to a decreasing ability of IHF to break the base pairs within it.

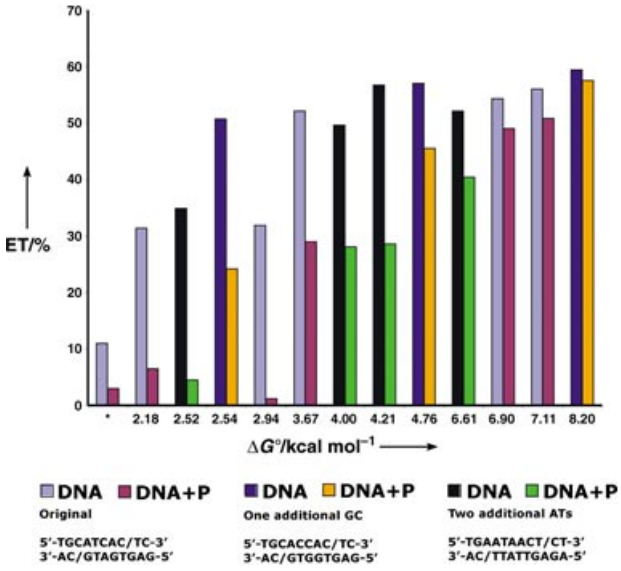

Figure 4. Donor energy transfer for molecules bound by IHF. The pairs of colored bars indicate the difference in energy transfer (ET) between unbound (DNA, left bar) and IHF-bound (DNA+P, right bar) forms. Three different overlap regions were used. The abscissa shows the estimated standard molar free energy available, based on a nearest-neighbor approximation.[8] Loop entropy was neglected. The differences are minimal at about 7–8 kcal mol^{-1}.

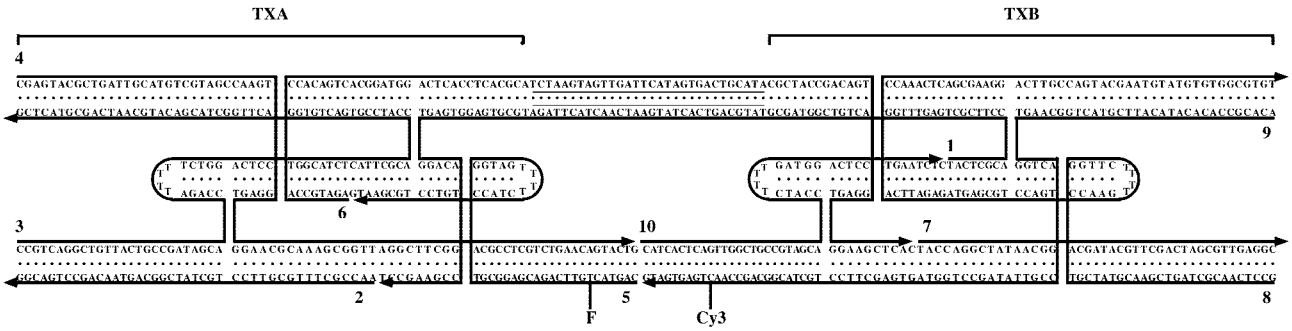

Figure 3. Sequence of the TX device used here. The ten individually numbered strands are indicated; arrowheads indicate the 3′ ends of the strands. The individual TX molecules are also indicated, and the IHF binding sequence is shown on strands 4 and 9 between them as an underlined region in the top helix. The site of fluorescein is indicated by F and that of Cy3 is shown similarly. Crossovers between strands are drawn as connections. A blunt-ended stack is shown in the bottom domain, but moving the nicks in the 3′ direction leads to the series of molecules used for the measurements. Variation of the sequence enables interpolation of values.

 © 2004 Wiley-VCH Verlag GmbH & Co. KGaA, Weinheim

indicates a nick] and changed the length of the overlap region systematically over a range of one to six nucleotide pairs. The donor energy transfers are plotted as light blue bars (before IHF binding) and light red bars (after IHF binding,). The abscissa corresponds to the standard free energy of the overlap region, using the parameters of ref. [8], plus others for the nicks, generously supplied by John SantaLucia. Each measurement was performed at least twice. Upon addition of IHF, the signal reporting energy transfer evolved for two minutes, and remained constant thereafter. We used two modifications of the basic sequence to supplement the values available from the initial sequence: data for [5′-TGCACCAC/TC-3′], containing one additional GC for AT substitution are shown in royal blue (unbound) and orange (bound), and those for [5′-TGAATAACT/CT-3′], containing two additional AT for GC substitutions, in black (unbound) and green (bound). We ascribe the relatively small amount of transfer before addition in the low-energy measurements to fraying of the small cohesive ends present. Nevertheless, it is clear that the energy transfer observed following addition of IHF increases as we increase the number of pairs holding the device together. The transition appears to be complete at about 7–8 kcal mol^{-1}, as indicated by the similar rates of energy transfer with and without IHF. We interpret the data for higher values of ΔG to indicate that the cohesion is too strong for the transition to occur.

The structures with a strand-disruption energy of less than 3 kcal mol^{-1} show little energy transfer when IHF is bound, while the structures with a disruption energy of 3–5 kcal mol^{-1} have an intermediate value for energy transfer in the presence of IHF. It is unlikely that this intermediate level comes from partial conversion of a device; these signals are more likely the average of a mixed population of completely disrupted molecules and intact molecules to which IHF was unable to bind. Once more than 7–8 kcal mol^{-1} is needed to disrupt the cohesive strands, essentially none of the devices are bent by IHF. Rather than selecting the midpoint of the measurement for our estimate of the amount of work that IHF can do, we selected the endpoint of the transition. The DNA base-pairing free energies provide only a crude indication of the energy. Yang and Nash[6] estimated the dissociation constant for IHF from the λH1 binding site to be 5.5 nM, a value for a system with no sticky ends to disrupt. Our measurement is independent of the value, and is the first estimate of the work IHF can do when it binds DNA.

We used IHF as a model DNA-bending protein to demonstrate that it is possible to use this nanomechanical device to perform the measurements described here. It is evident that this same system could be used to characterize the amount of work that can be done by other DNA-bending proteins. However, for proteins that bend in the opposite direction, such as TATA binding protein (TBP),[9] motifs with more than three coplanar helices may be needed. The question arises whether it would be possible to measure the amount of work available from proteins that introduce other distortions of DNA, such as twisting. We intentionally made this device sensitive to the relatively small spatial displacements associated with rotations. Thus, we replaced the DX units we used in the related B–Z device[2] with TX units; consequently, a twisting displacement as small as 60° leads to a change in distance (observed as a change in FRET) as large as that associated with the 180° rotation of the B–Z device. For example, the postulated twisting of SoxR[10] could be examined if its iron sulfur cluster did not quench the dyes.

Experimental Section

DNA sequences were designed with SEQUIN,[11] synthesized by standard phosphoramidite techniques,[12] and purified from denaturing gels. Cy3 labeling was done by filling-in Cyanine 3-dCTP (PerkinElmer) with Klenow Fragment (NEB) polymerase, by following a protocol suggested by the supplier. IHF was prepared as described previously.[13] 50 μM IHF stock solutions were added to aliquots of 100 μL of 100 nM DNA device complexes up to a final IHF concentration of 300 nM and incubated for 10 min before each measurement. Steady-state fluorescence measurements were performed with an AMINCO BOWMAN Series 2 spectrometer at room temperature. The emission spectra were corrected for instrument response, lamp fluctuations, and buffer contributions; energy transfer was performed as described previously.[2]

Received: April 13, 2004

Keywords: DNA structures · fluorescent probes · molecular devices · proteins

[1] X. Yang, A. Vologodskii, B. Liu, B. Kemper, N. C. Seeman, *Biopolymers* **1998**, *45*, 69–83.
[2] C. Mao, W. Sun, Z. Shen, N. C. Seeman, *Nature* **1999**, *397*, 144–146.
[3] H. Yan, X. Zhang, Z. Shen, N. C. Seeman, *Nature* **2002**, *415*, 62–65.
[4] P. A. Rice, S. W. Yang, K. Mizuuchi, H. A. Nash, *Cell* **1996**, *87*, 1295–1306.
[5] T. LaBean, H. Yan, J. Kopatsch, F. Liu, E. Winfree, J. H. Reif, N. C. Seeman, *J. Am. Chem. Soc.* **2000**, *122*, 1848–1860.
[6] S. W. Yang, H. A. Nash, *EMBO J.* **1995**, *14*, 6292–6300.
[7] W. Shen, PhD Thesis, New York University, **2004**.
[8] J. SantaLucia, *Proc. Natl. Acad. Sci. USA* **1998**, *95*, 1460–1465, and references therein.
[9] Y. C. Kim, J. H. Geiger, S. Hahn, P. B. Sigler, *Nature* **1993**, *365*, 512–520.
[10] E. Hidalgo, B. Demple, *EMBO J.* **1997**, *16*, 1056–1065.
[11] N. C. Seeman, *J. Biomol. Struct. Dyn.* **1990**, *8*, 573–581.
[12] M. H. Caruthers, *Science* **1985**, *230*, 281–285.
[13] S. D. Goodman, S. C. Nicholson, H. A. Nash, *Proc. Natl. Acad. Sci. USA* **1992**, *89*, 11910–11914.

 © 2004 Wiley-VCH Verlag GmbH & Co. KGaA, Weinheim